

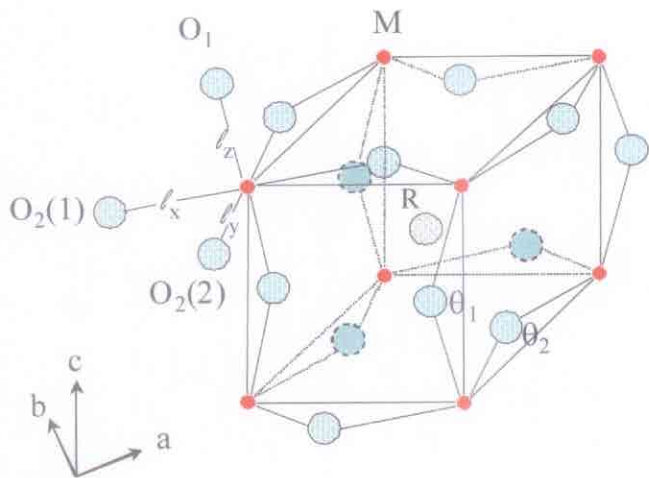
Magnetic properties of perovskites with d-orbital degeneracies

J.-S. Zhou and J.B. Goodenough

Texas Materials Institute, University of Texas at Austin

1. Universal octahedral-site distortion in orthorhombic RMO_3 perovskites.
2. RTiO_3
3. RVO_3
4. RMnO_3
5. $\text{A}^{2+}\text{Ru}^{4+}\text{O}_3$

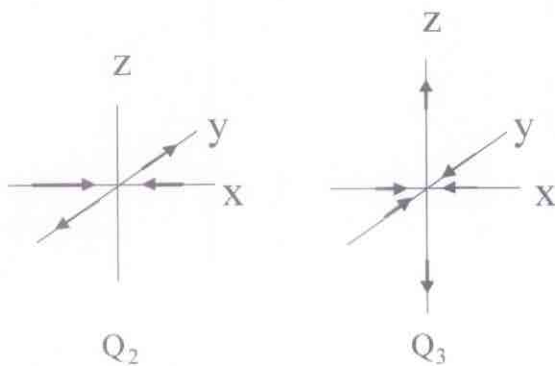
The crystal structure of orthorhombic RMO_3 perovskites



The basic perovskite unit cell with the orthorhombic distortion with Pbnm space group.

Coop. rotation about [110], [001]
 $\rightarrow a \leq c/\sqrt{2} < b$

Problem: Need $\text{MO}_{6/2}$ site distortion to accommodate fixed rotation axis.
O'Keeffe & Hyde (1977)



$$Q_2 = \ell_x - \ell_y, \quad Q_3 = (2\ell_z - \ell_x - \ell_y)/\sqrt{3},$$

$$\rho_o = (Q_2^2 + Q_3^2)^{1/2} \text{ and } \phi = \tan^{-1}(Q_3/Q_2)$$

IR = R^{3+} -ion radius (9-fold coordination)

Calculated vs Experimental ω and α

SPuDS program is used for calculating ω vs IR
Lufaso & Woodward, Acta Cryst. B 57, 725 (2001)

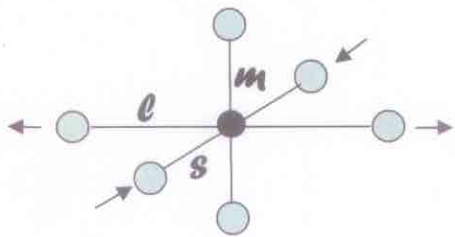
Assumes:

- (1) Rigid $\text{MO}_{6/2}$ rotations
- (2) (M-O) from bond valance sum rule.

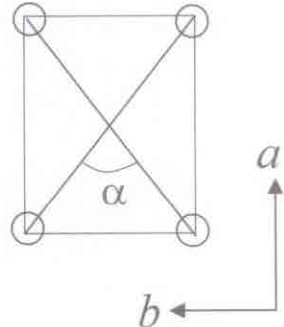
Experiments:

RFeO_3 (Pbnm for all R), *Marezio et al, Acta Cryst. B 26, 2008 (1970)*
Mat. Res. Bull. 6, 23 (1971).

Apparent octahedral-site distortions:



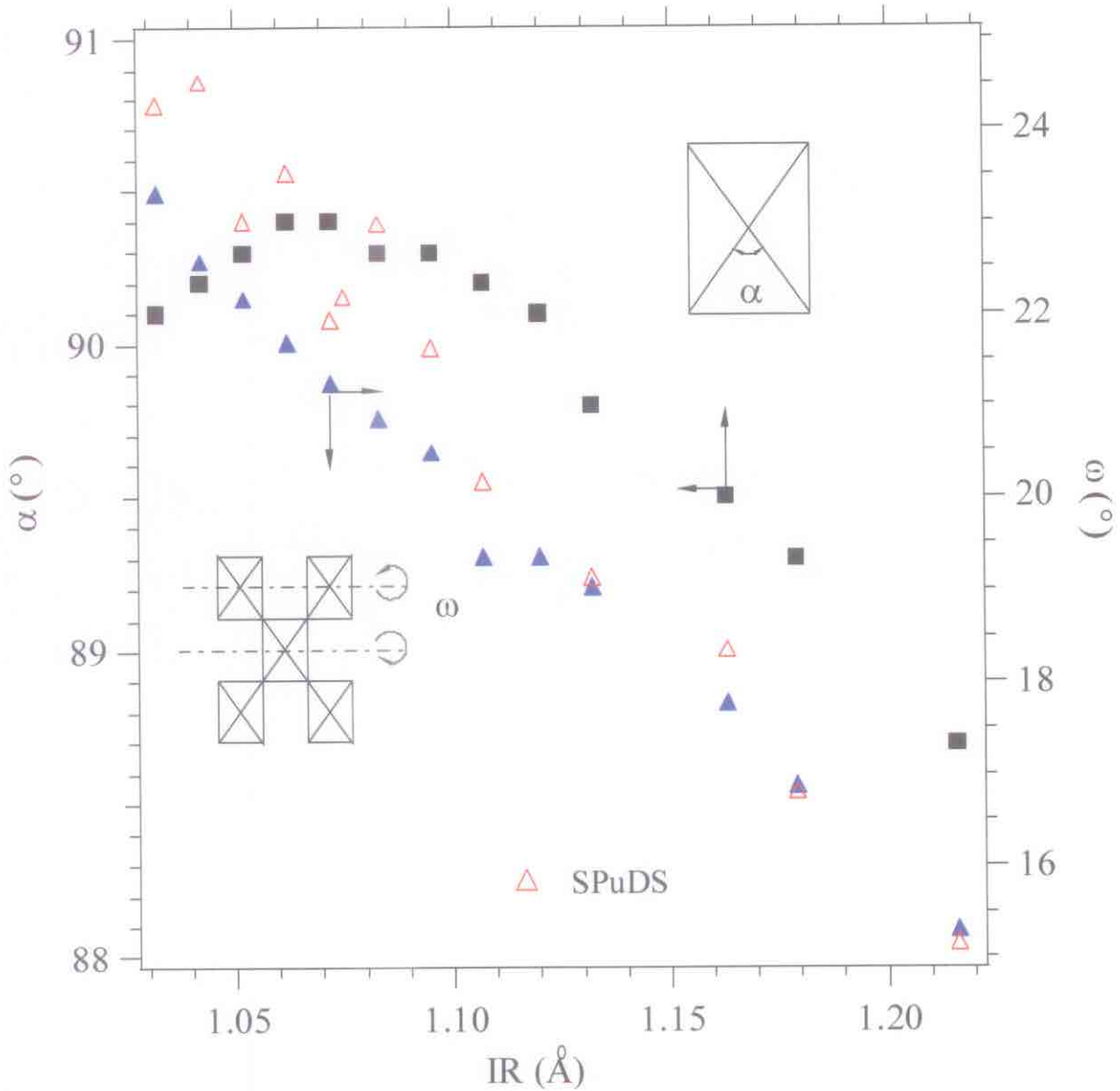
Max. distortion @ IR $\approx 1.11 \text{ \AA}$

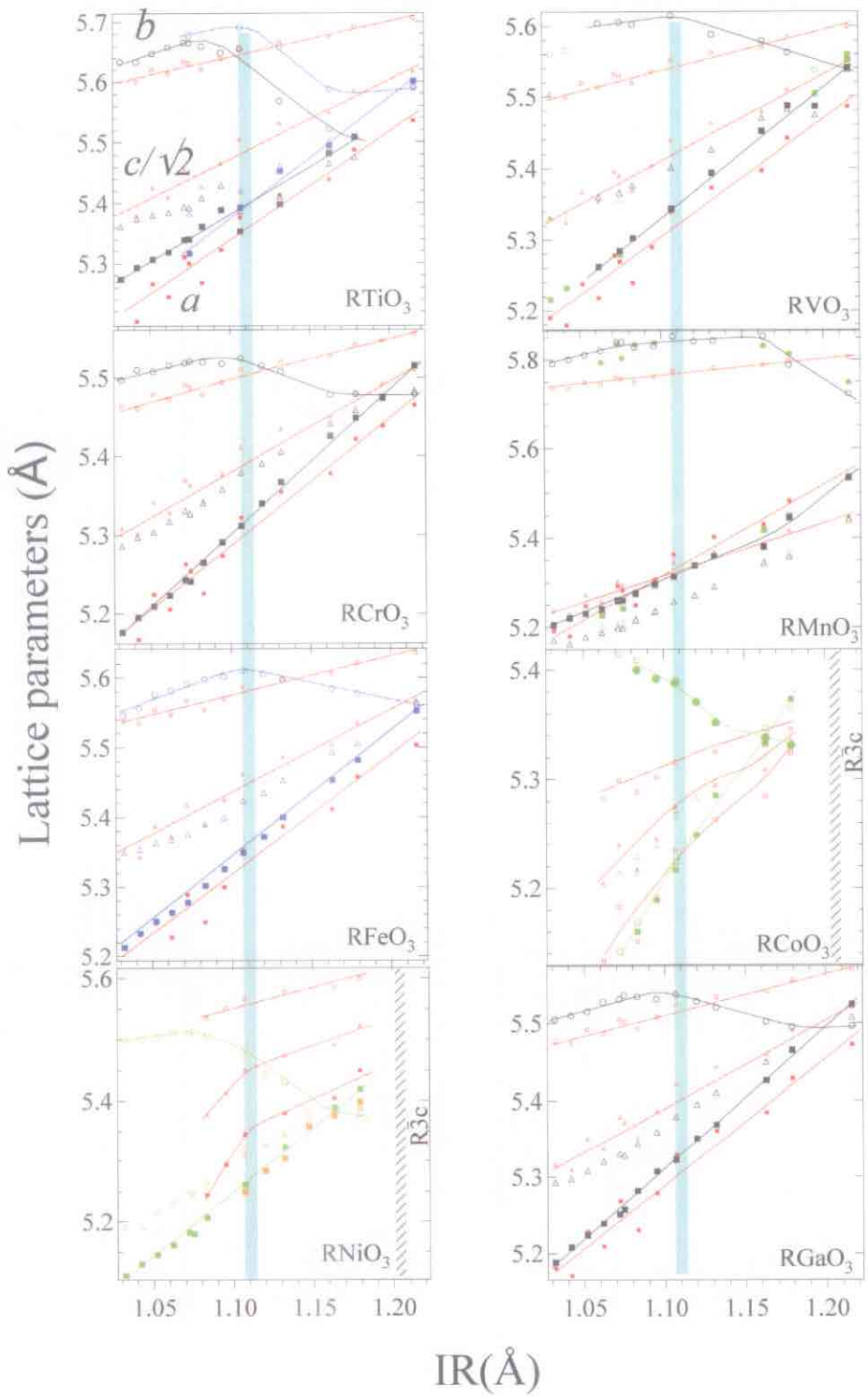


$\alpha < 90^\circ$ for IR $> 1.11 \text{ \AA}$

Note: With increasing IR,
Ortho (Pbnm) \longrightarrow Rhomb ($\bar{R}3c$) \longrightarrow Cubic (Pm3m)
The rhombohedral structure accommodates larger IR.

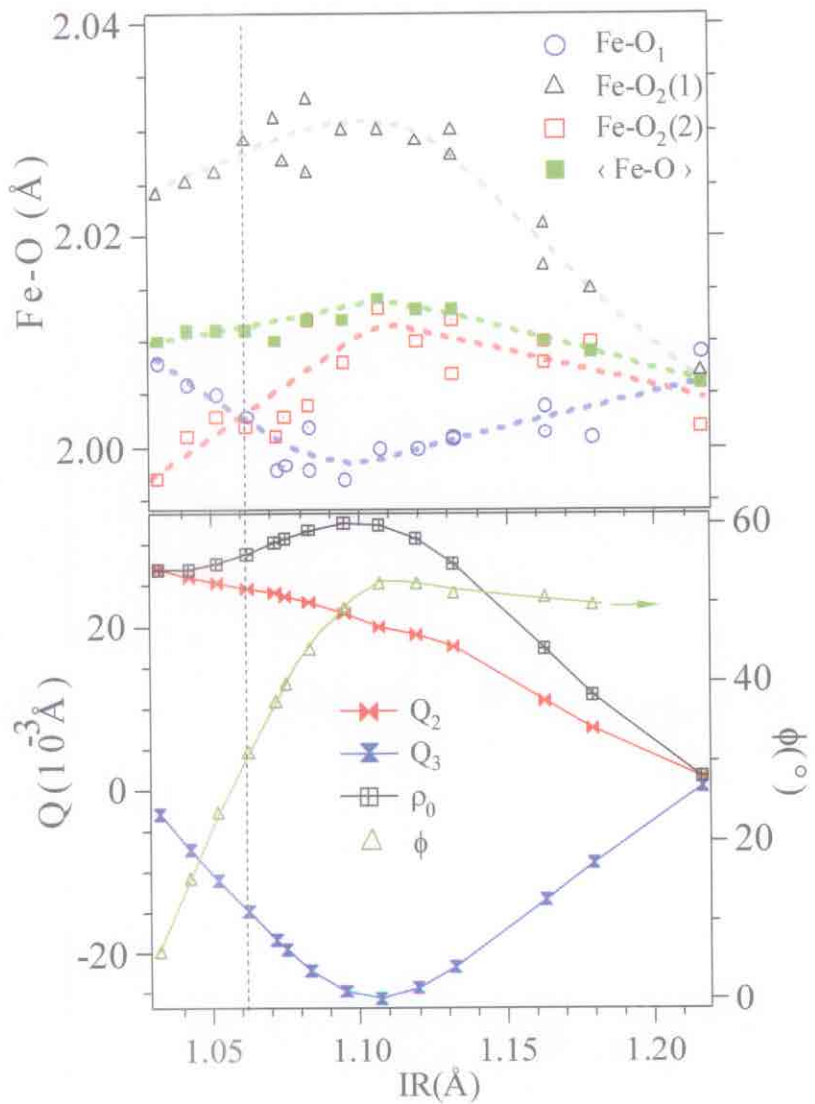
Angles ω and α vs. IR for RFeO₃ (Data from Marezio et al)



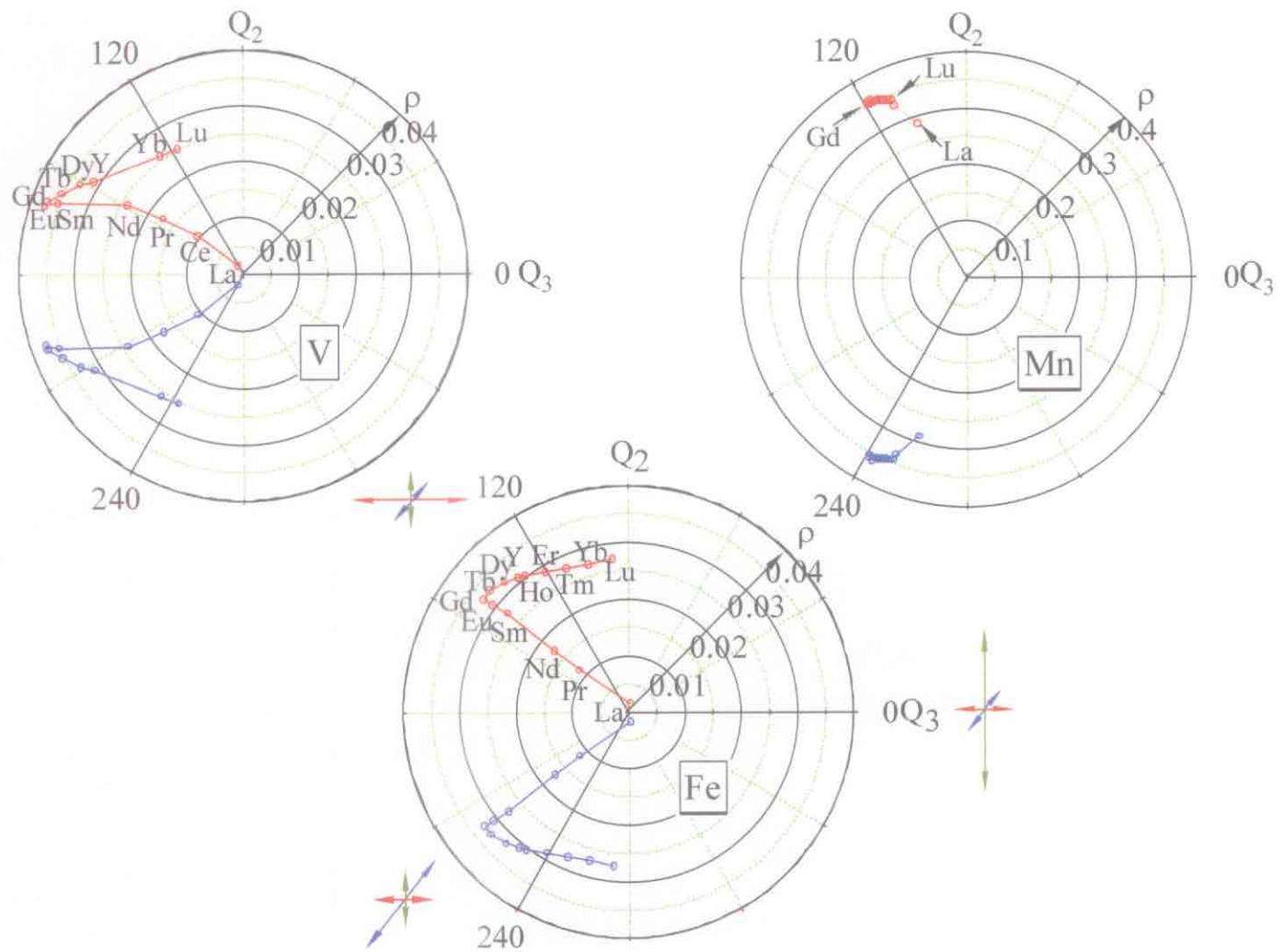


Lattice parameters with red symbols are calculated by SPuDS

Fe-O bond lengths in RFeO₃



Note: $\phi = \tan^{-1}(Q_3/Q_2) = 30^\circ$
 for the octahedral-site distortion c/a > 1

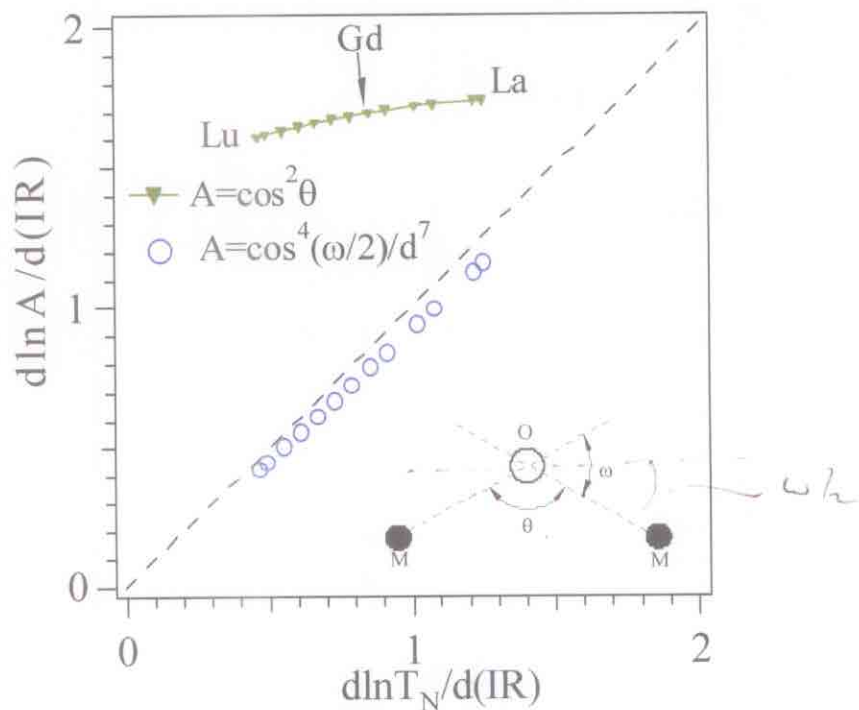


$$Q_2 = \ell_x - \ell_y, \quad Q_3 = (2\ell_z - \ell_x - \ell_y)/\sqrt{3},$$

$$\rho_o = (Q_2^2 + Q_3^2)^{1/2} \text{ and } \phi = \tan^{-1}(Q_3/Q_2)$$

T_N observed vs the calculated value from superexchange interaction for $RFeO_3$

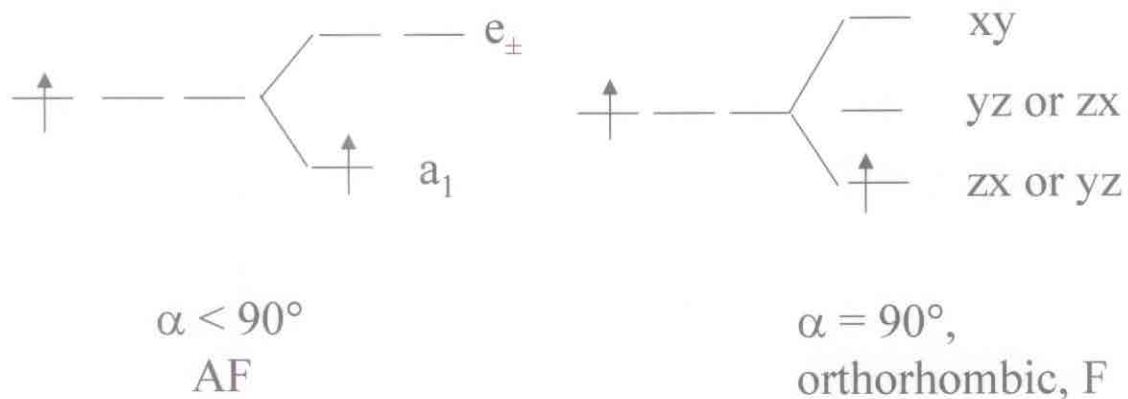
Superexchange: $T_N \sim b^2/U \sim A(\theta, d)$;
 θ : Fe-O-Fe bond angle; d : Fe-O bond length.
For fixed U and $A \sim b^2$
→ $d\ln A/d(\text{IR})$ vs $d\ln T_N/d(\text{IR})$ is straight line at 45° through origin.
 $A(\text{IR})$ from the structural data, $T_N(\text{IR})$ from Mössbauer data.



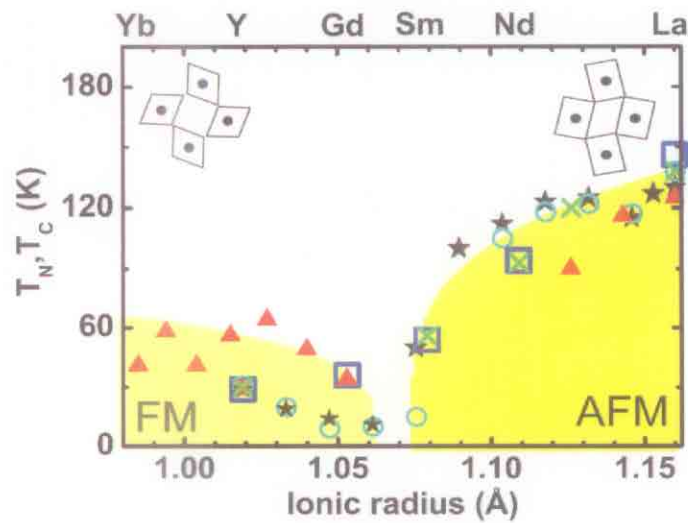
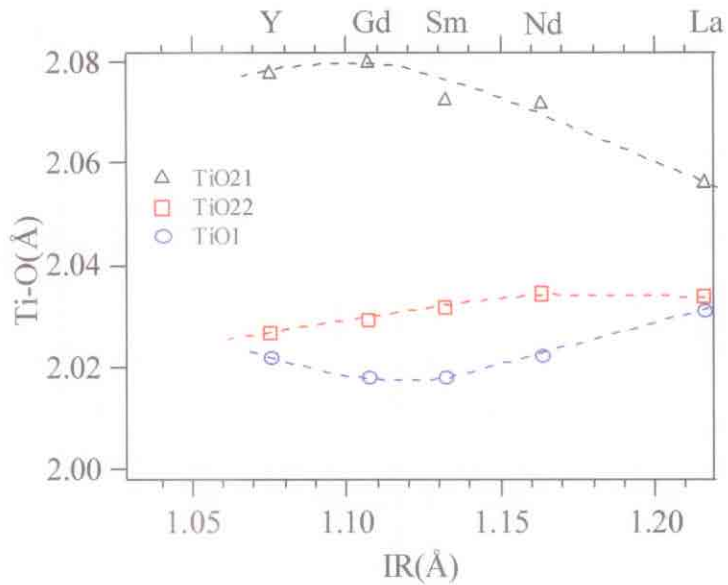
The RTiO₃ Perovskites

Ti³⁺:t¹σ*⁰

Possible site orbital order



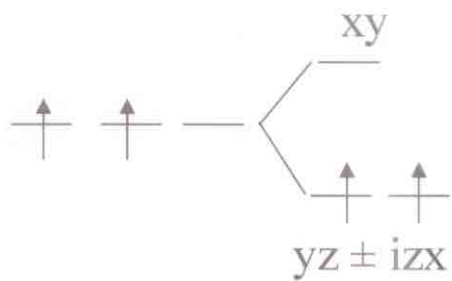
RTiO_3



A.C. Komarek *et al* PRB **75**, 224402(2007)

RVO₃ perovskites V³⁺:t²e⁰: localized spins

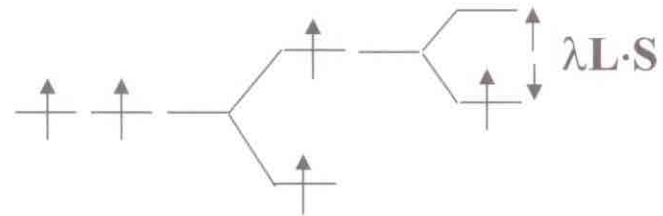
Possible site orbital order



Tetr c/a >1

$$T_{OO} > T_N$$

Cooperative antiferroic



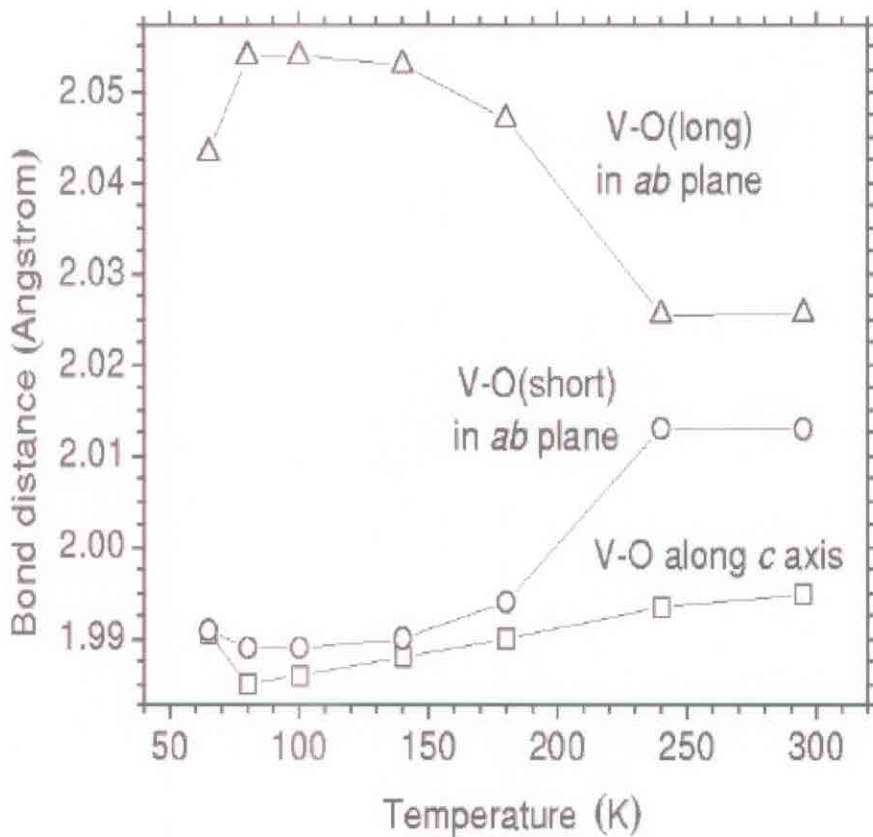
Pseudocubic (c/a ≈ 1)

$$T_{OO} \leq T_N ?$$

Cooperative ferroic

YVO_3 site distortion

Note: Distortion at $T > T_{\text{OO}}$ largest for $\text{IR} \approx 1.11 \text{ \AA}$



Temperature dependence of V-O bond lengths determined by using neutron powder diffraction.
Blake et al *Phys. Rev. B* 65, 174112 (2002)

Orbital & Spin ordering in YVO₃

Orbital ordering and spin-spin interactions:

G_{OO}: T_{CG} < T < T_{OO}

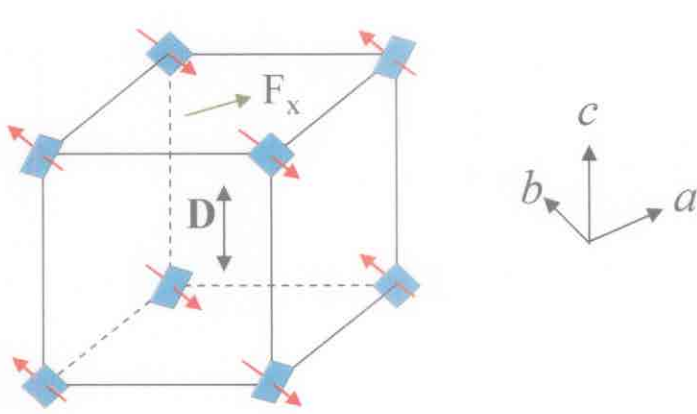
C_{OO}: T < T_{CG}

AF: xy¹-xy¹, yz¹-yz¹, zx¹-zx¹

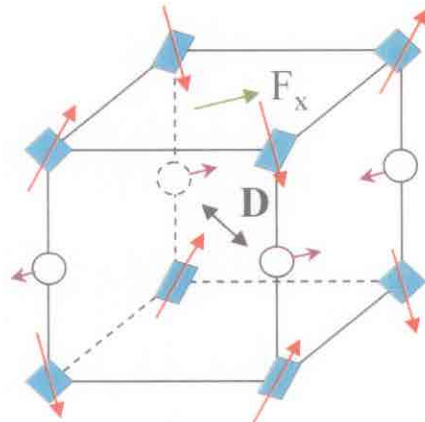
F: yz¹-yz⁰, zx¹-zx⁰



G_{OO}C_{SO}: T_{CG} < T < T_N
C_{OO} G_{SO}: T < T_{CG}



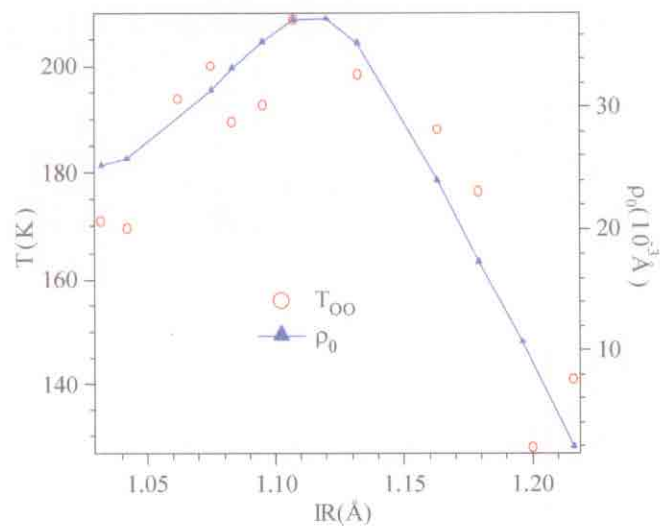
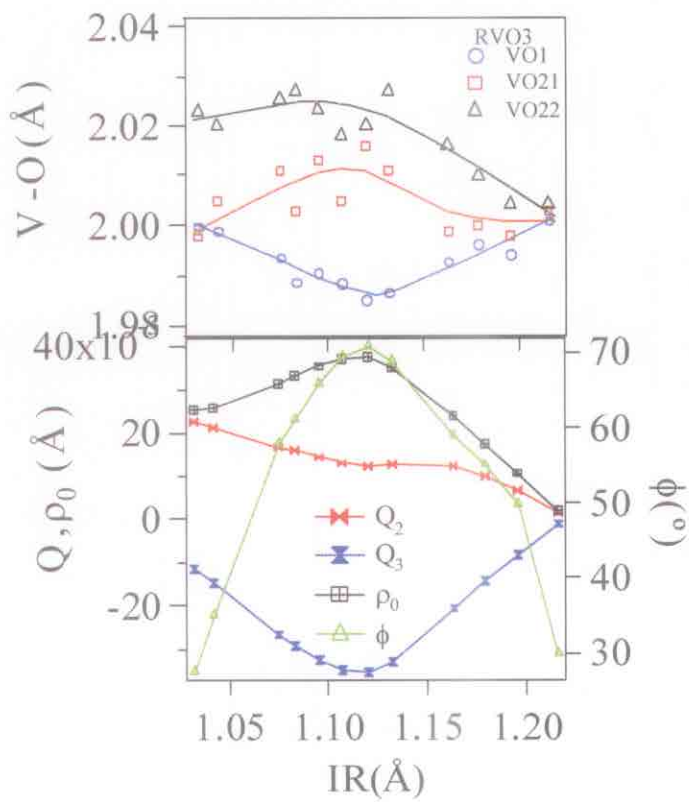
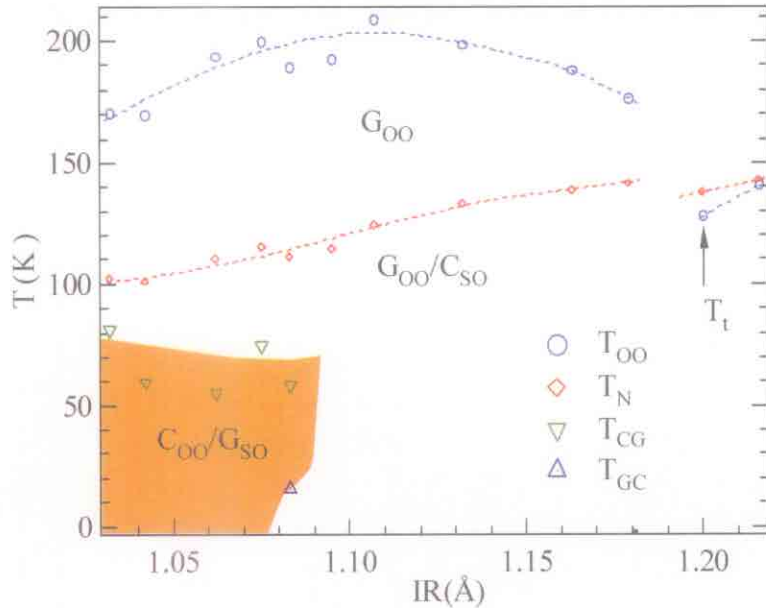
T_{CG} < T < T_N
C_yF_x



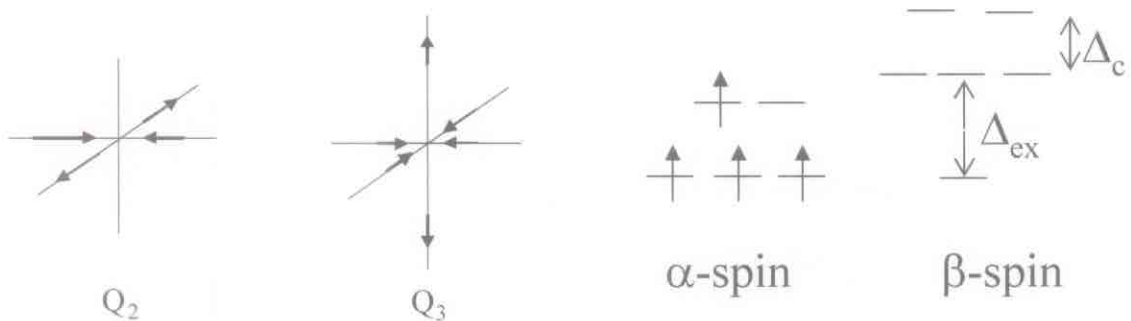
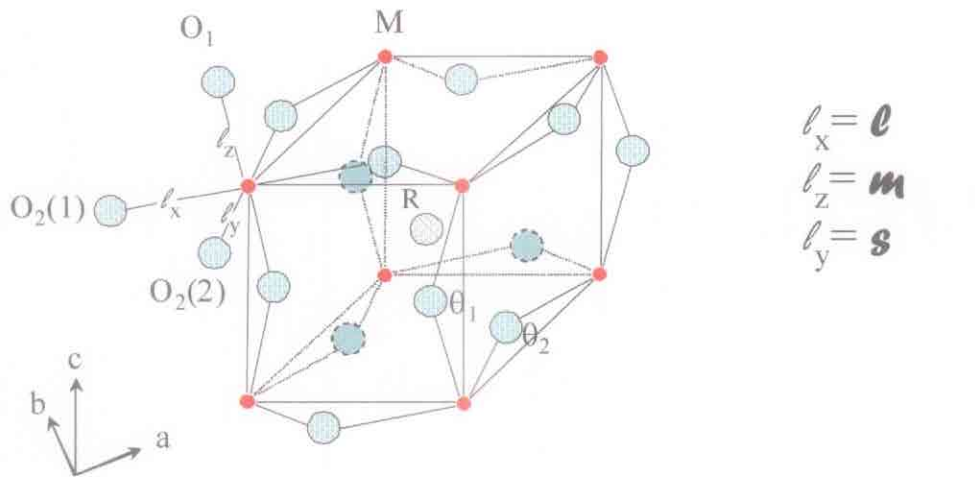
T < T_{CG}
G_zF_x

$\mathbf{D}_{ij} \cdot \mathbf{S}_i \times \mathbf{S}_j$ gives F_x
VO_{6/2} rotations also give F_x for T < T_{CG}

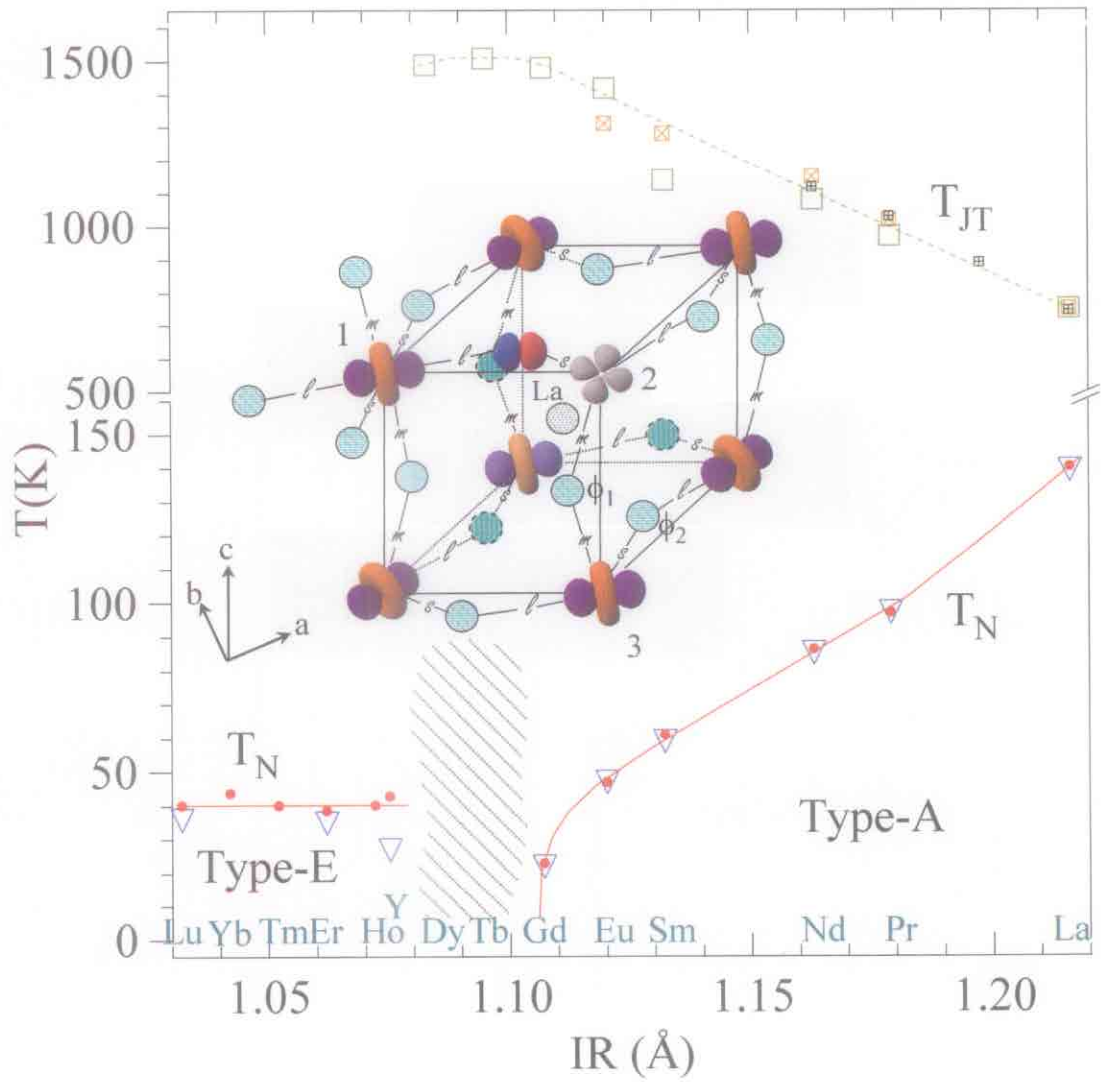
RVO₃



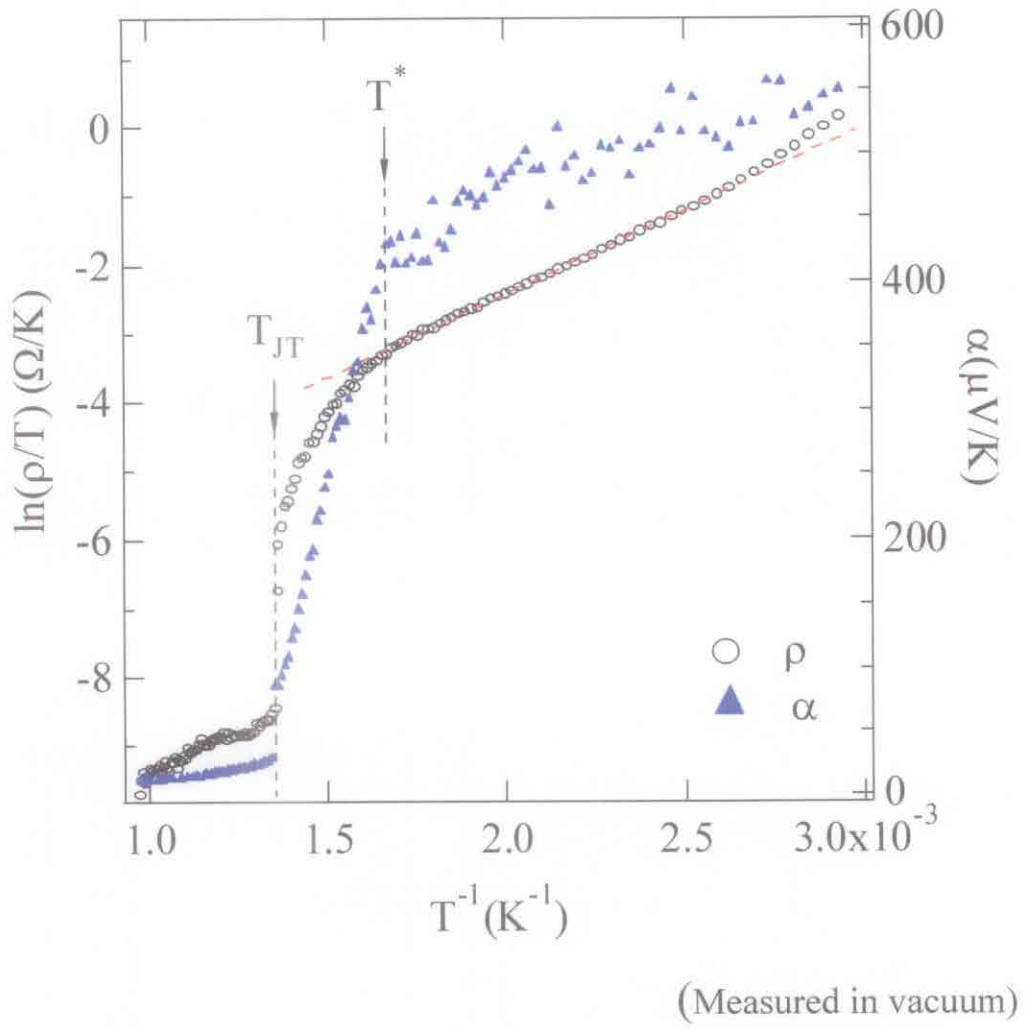
Jahn-Teller deformation in RMnO₃



RMnO_3



LaMnO₃



$T > T_{JT}$: Orbital disorder
 Partial $2\text{Mn}^{3+} \rightarrow \text{Mn}^{2+} + \text{Mn}^{4+}$

$T^* < T < T_{JT}$: short-range orbital disorder

Mn-O-Mn Superexchange

c axis: e⁰-O-e⁰ (AF) & t³-O-t³ (AF)

a-b plane: t³-O-t³ (AF) & e¹-O-e⁰ (F)

For type-A magnetic order

$$T_N \sim b_\sigma^2 / \Delta_\sigma$$

Where

$$b_\sigma^2 \sim \cos^4(\gamma/2) \cos^4(\omega/2) |(3x^2 - r^2)| H' |(x^2 - z^2)|^2$$

$$\Delta_\sigma \approx \Delta_{JT} \sim kT_{JT}$$

$$\gamma = 30^\circ - \tan^{-1}(Q_3/Q_2)$$

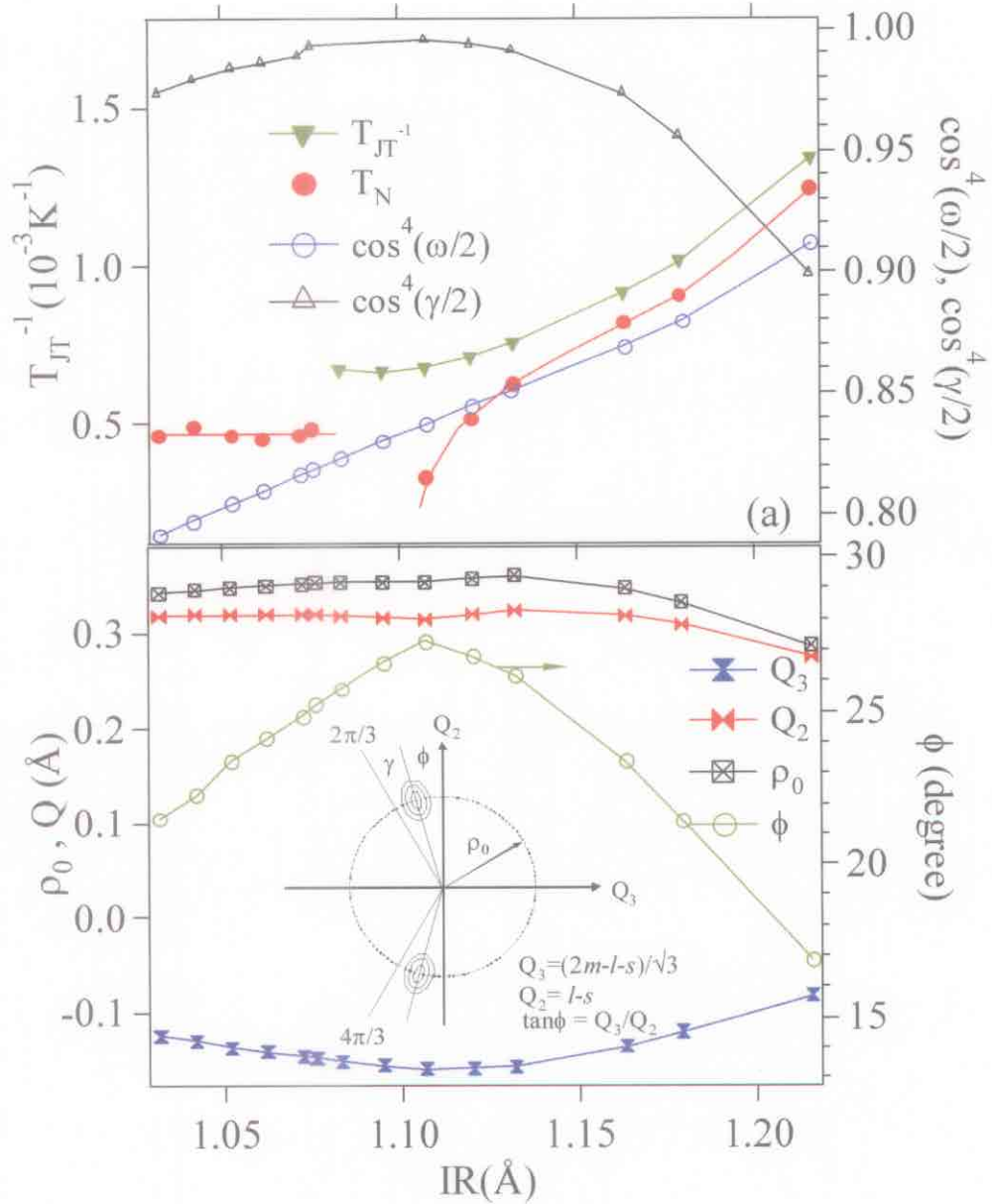
Note:

(1) $d[\ln \cos^4(\omega/2)]/d(IR) : d\ln T_N/d(IR) = 0.8 : 9$

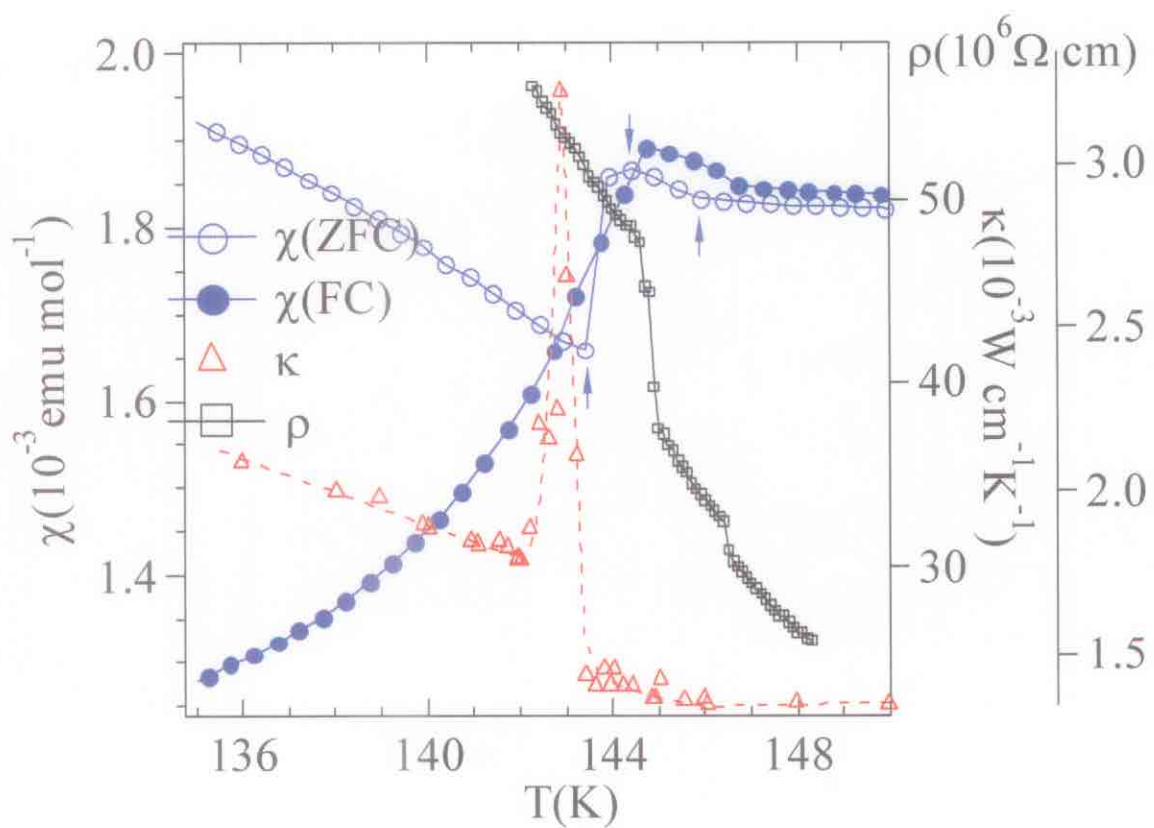
(2) $d[\ln \cos^4(\gamma/2)]/d(IR)$ is negative, whereas $d\ln T_N/d(IR)$ is positive.

(3) $d[\ln(1/T_{JT})]/d(IR) : d\ln T_N/d(IR) = 7 : 9$

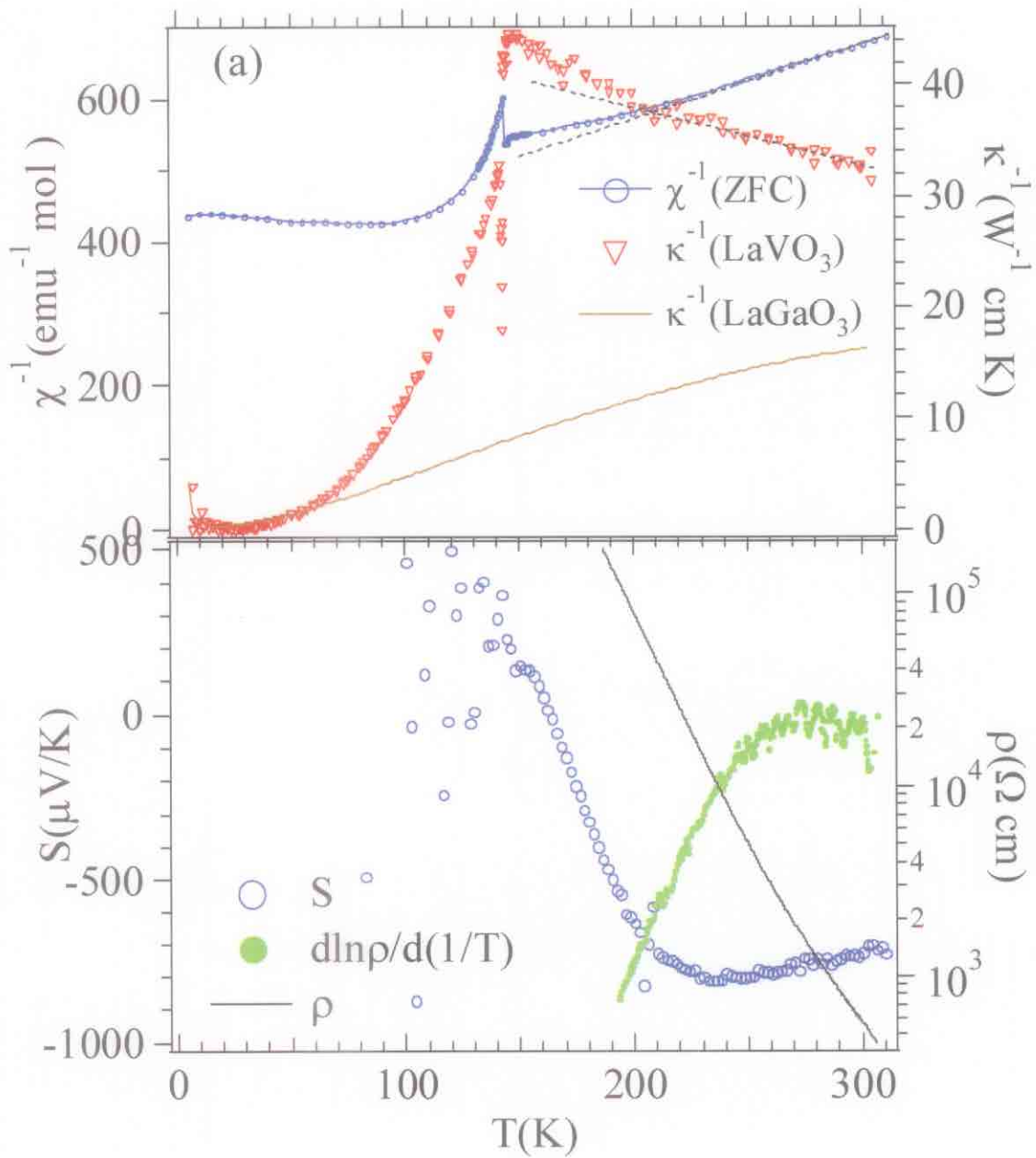
RMnO₃



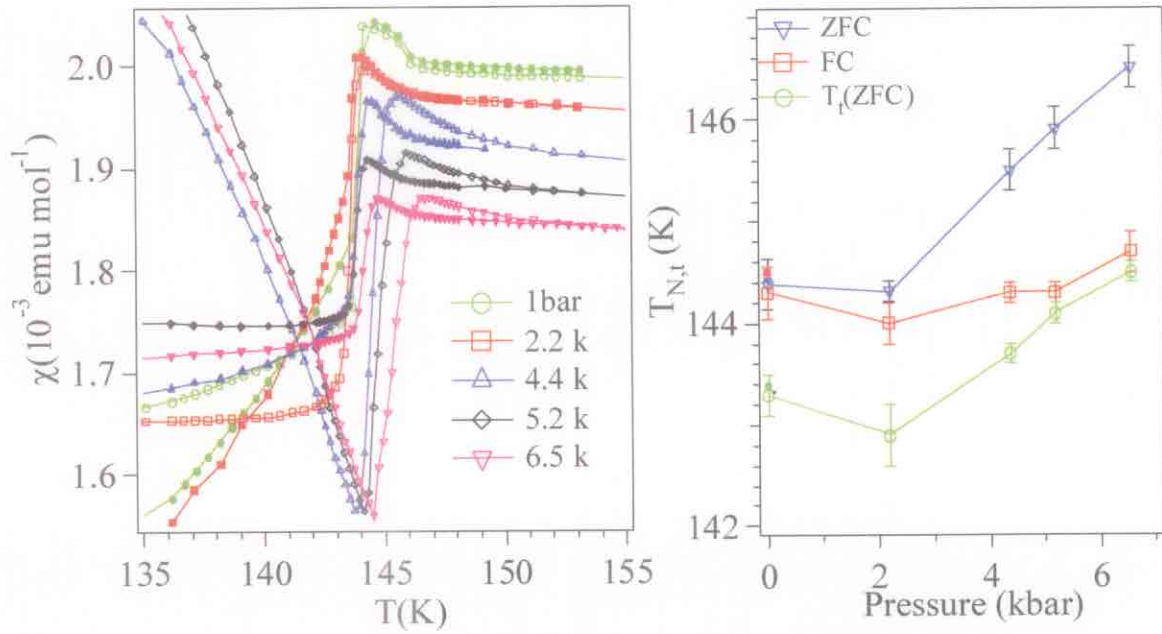
LaVO₃



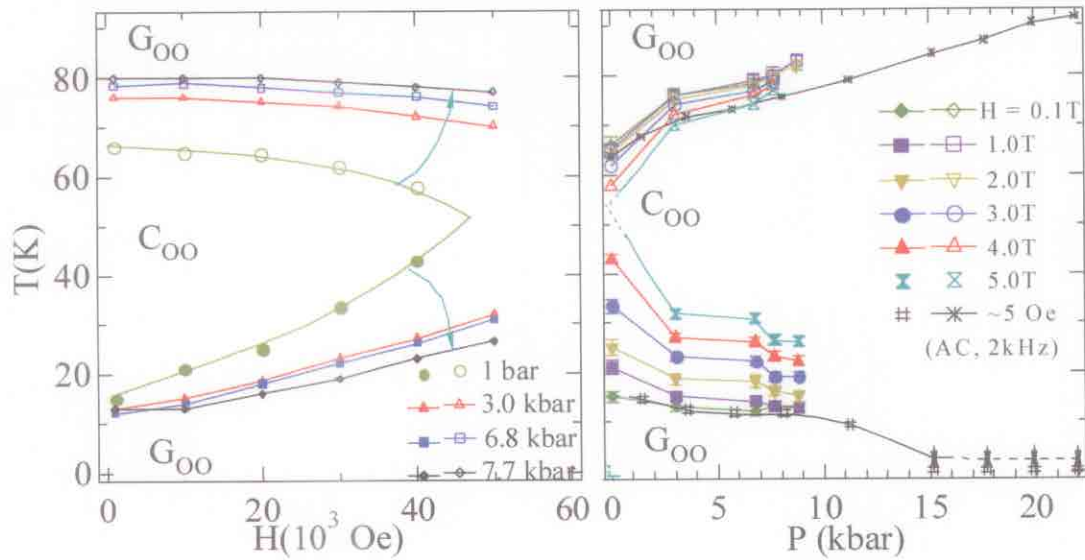
LaVO₃



LaVO₃



DyVO₃

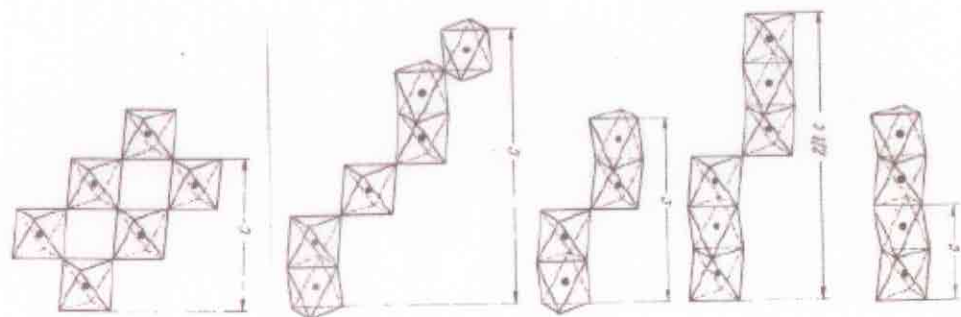
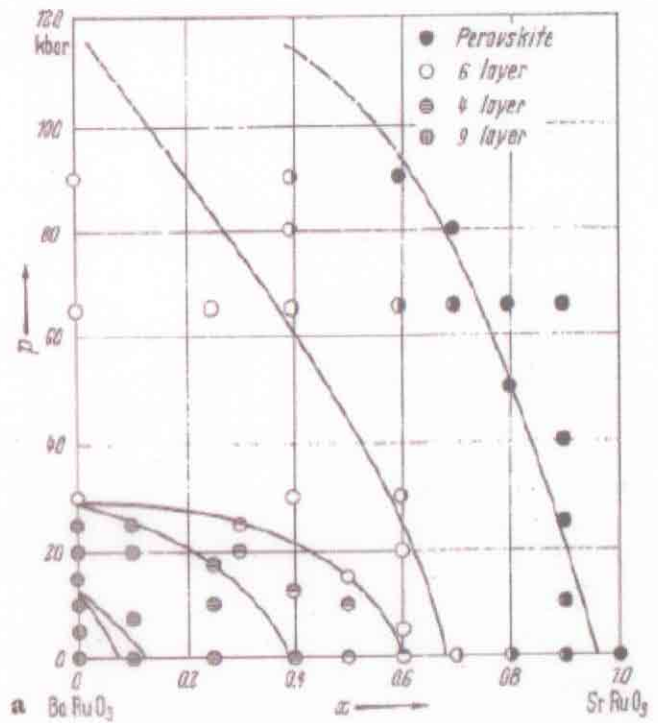


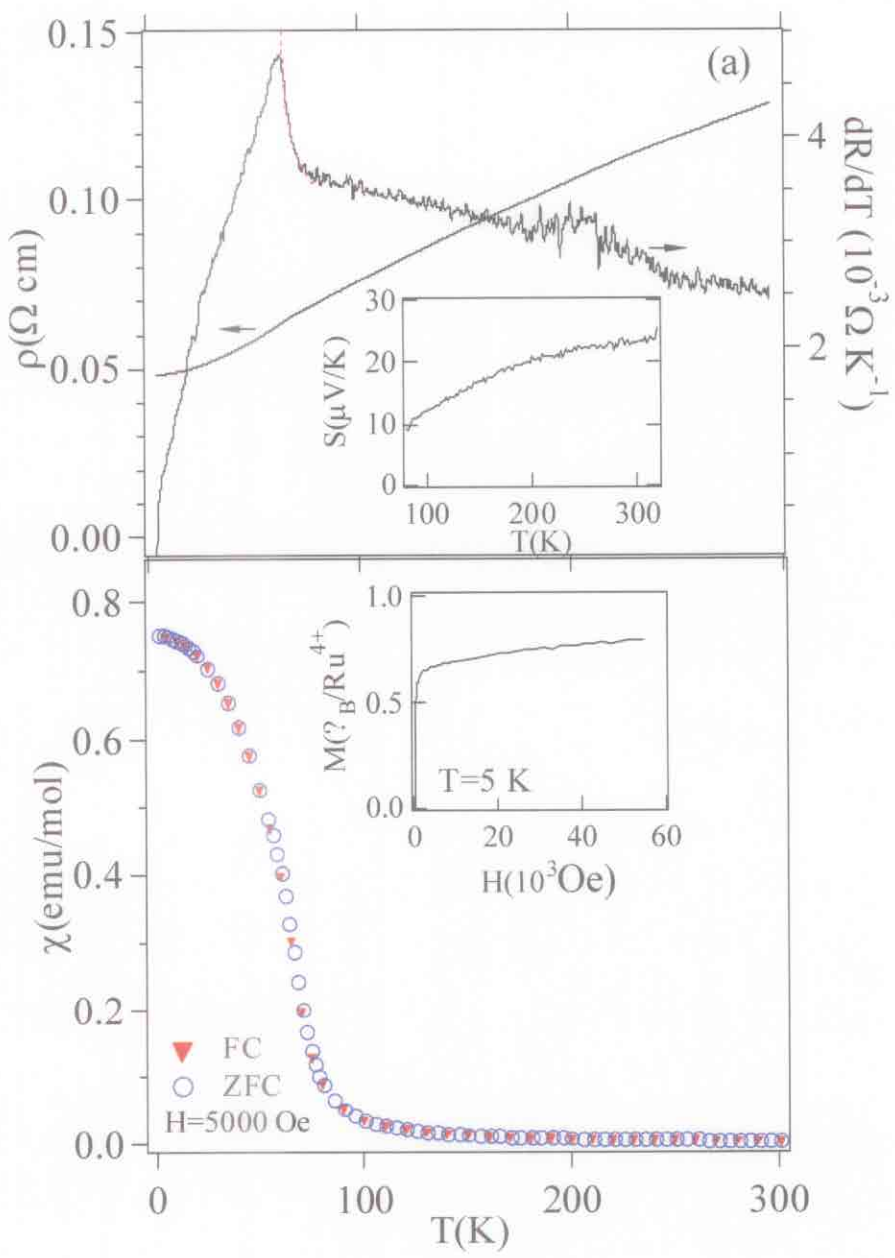
$\text{Sr}_{1-x}\text{Ca}_x\text{RuO}_3$

SrRuO₃: Itinerant-electron ferromagnet
Low-spin Ru⁴⁺: $\pi^* 4\sigma^{*0}$
 $T_c = 164 \text{ K}$, $\mu_{\text{Ru}} = 1.4 \mu_B$ @ 5 K
 $\mu_{\text{eff}} = 2.6 \mu_B/\text{Ru}$
($S = 1 \mu_{\text{eff}}$ (spin-only) = $2.8 \mu_B/\text{Ru}$)

Sr_{1-x}Ca_xRuO₃: Weiss $\theta > T_c$ for $x = 0$ decreases faster than T_c with increasing x . $T_c \rightarrow 0$ and θ changes sign at $x \approx 0.8$

CaRuO₃: No long-range magnetic order.
Ti⁴⁺ substitution shows CaRuO₃ on verge of ferromagnetic order
[Cava & He, *Phys. Rev. B* **63**, 172403 (2001)]

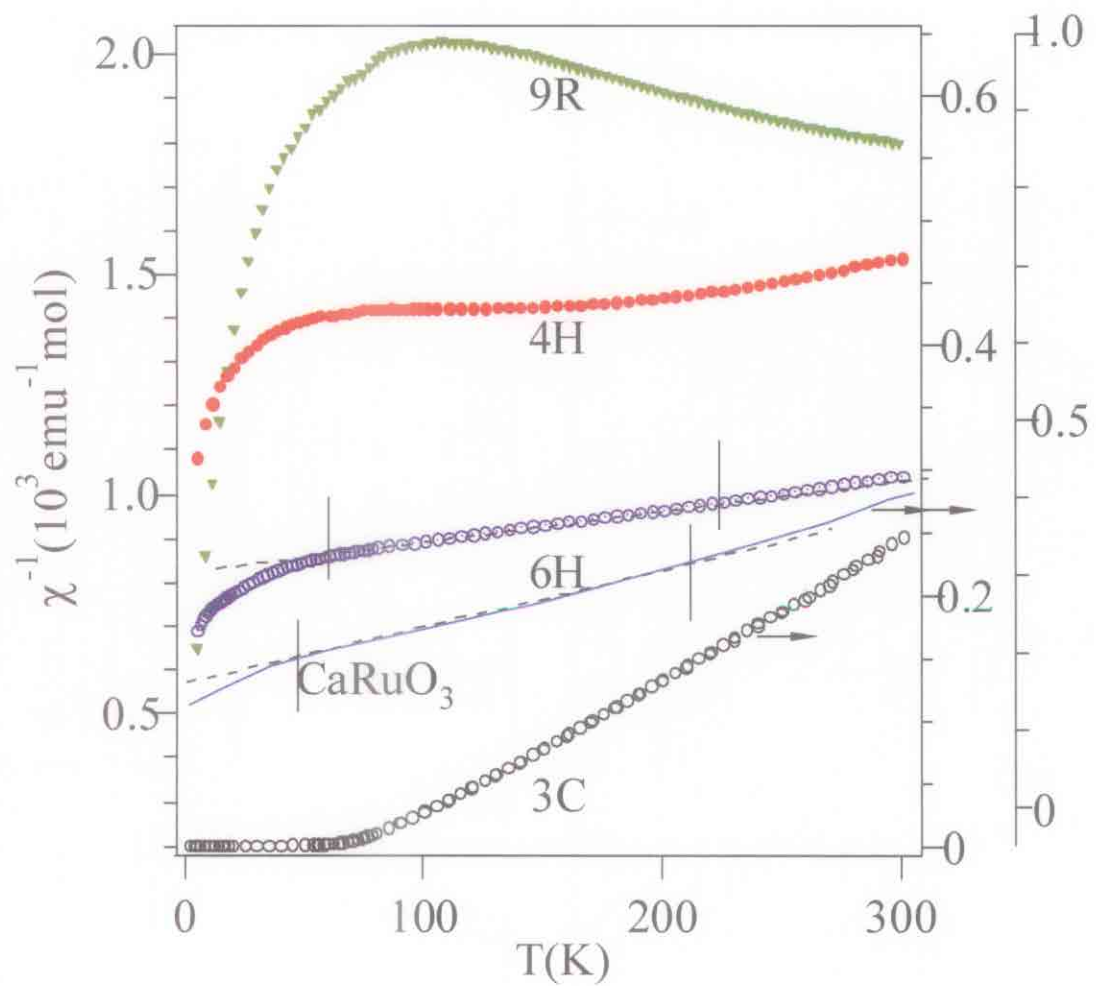


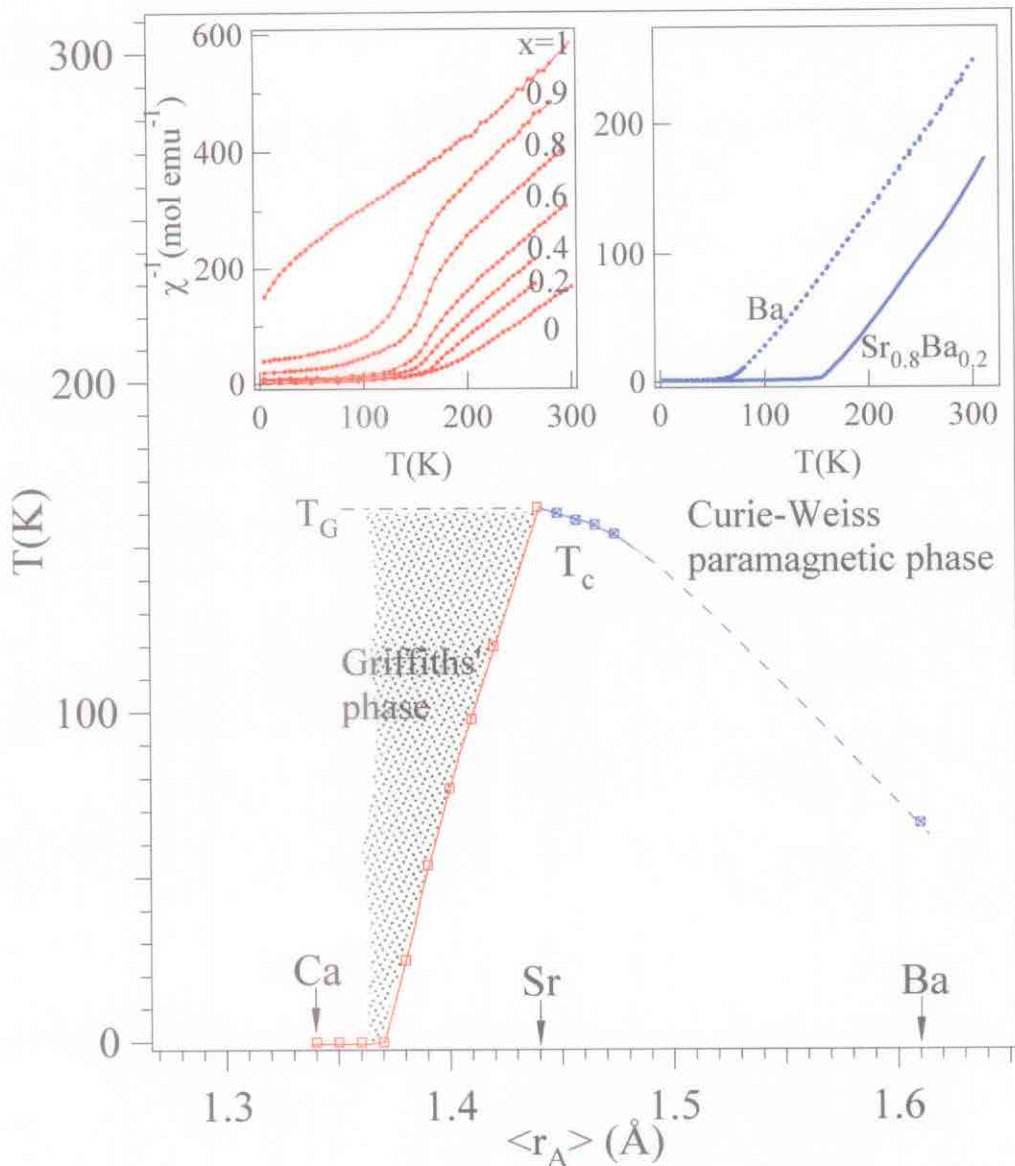


**Cubic BaRuO₃: 1100°C @ 18 GPa KAWAI
mutianvil press C.-Q. Jin *et al* (unpublished)**

9R: Dillon *et al*, J. Chem. Soc. Faraday Transactions 75, 1193 (1979)

CaRuO₃: Yashimura *et al*, Phys. Rev. Lett. 83, 4397 (1999)





C.-Q. Jin *et al* (unpublished)

Conclusions:

- Acidity of A-O bond: $Ca > Sr > Ba$
- Intraatomic $\lambda L \cdot S$ on a Ru^{4+} ion suppresses the interatomic spin-spin interaction in neighborhood of Ca.